

Use of ICG-guided fluorescence imaging in pediatric laparoscopic and robot-assisted surgery: a single-center retrospective study

Ciro Esposito^a, Mariapina Cerulo^a, Francesca Carraturo^a, Fulvia Del Conte^a, Claudia Di Mento^a, Vincenzo Coppola^a, Giovanni Esposito^b, Francesco Tedesco^a, Valerio Mazzone^a, Annalisa Chiodi^a, Maria Escolino^{a,*}

^a Division of Pediatric Surgery, Federico II University Hospital, via Pansini, 5, 80131, Naples, Italy.

^b CEINGE Advanced Biotechnology, Via Gaetano Salvatore, 486, 80131, Naples, Italy.

This article belongs to the Special Issue: [Use of imaging technologies for robot-assisted surgery](#)

Abstract

Background: Indocyanine green (ICG) fluorescence imaging represents a recent advancement in pediatric minimally invasive surgery (MIS), offering superior visualization of critical anatomical structures. Despite its growing application, evidence on its specific utility in pediatric urology remains limited. This study aimed to evaluate the safety, efficacy, and broader applications of ICG-guided fluorescence imaging in pediatric robotic and laparoscopic surgery, with an emphasis on refining surgical precision and improving outcomes. Building on our previous research on ICG applications, this work expands the focus to include a larger cohort and a diverse range of procedures to establish standardized protocols.

Methods: The records of all patients undergoing robotic or laparoscopic urological surgery with ICG-NIRF assistance over a 7-year period (2018–2024), were analyzed retrospectively. ICG was administered using tailored protocols for each procedure type, with fluorescence imaging applied to enhance intraoperative navigation and decision-making. The ICG dosage ranged between 0.035 and 0.5 mg/kg.

Results: Patient cohort included 278 patients with median age of 9.2 years (range 1-18). Laparoscopic procedures with ICG-NIRF were performed in 181 patients (65.1%), including pyeloplasty ($n = 11$), varicocelectomy ($n = 118$), adnexal pathology resection ($n = 33$), partial nephrectomy ($n = 10$), nephrectomy ($n = 6$), and urachal cyst excision ($n = 3$). The remaining 97 patients (34.9%) underwent robot-assisted procedures, including pyeloplasty ($n = 22$), varicocelectomy ($n = 34$), adnexal pathology resection ($n = 17$), partial nephrectomy ($n = 4$), nephrectomy ($n = 4$), excision of periureteral diverticulum and dismembered extravesical ureteral reimplantation ($n = 13$), renal cyst removal ($n = 2$), and prostatic utricle cyst excision ($n = 1$). All procedures were completed successfully without conversions to open surgery. Clear visualization of target anatomy was achieved in all cases, with no intraoperative complications. The median hospital stay was 2.7 days (range 1-7). The complication rate (Clavien 3b) was 0.7%, with no allergic reactions reported.

Conclusion: The findings of this study highlight the potential of ICG fluorescence as an innovative tool in the pediatric urology field. While the current evidence supports its safety, feasibility, and ability to enhance intraoperative visualization, prospective, controlled trials are needed to validate its efficacy, investigate functional outcomes, and compare its utility with existing standard practices.

Keywords: ICG, fluorescence, robotics, laparoscopy, urology, imaging, pediatrics

* Corresponding author: Maria Escolino

Mailing address: Division of Pediatric Surgery Federico II University Hospital, Via Pansini 5, 80131 Naples, Italy.

Email: x.escolino@libero.it

Received: 07 December 2024 / Revised: 19 December 2024

Accepted: 08 January 2025 / Published: 26 March 2025

Introduction

Indocyanine green (ICG) fluorescence imaging has been recently introduced in the field of pediatric minimally invasive surgery (MIS), due to its ability to provide real-

time, high-contrast imaging of anatomical structures [1-3]. Its application in pediatric urology can potentially address the inherent challenges posed by smaller anatomical structures, complex congenital anomalies, and the necessity for minimally invasive approaches in children [4, 5]. The use of ICG fluorescence technology has been authorized for clinical application by both the Food and Drug Administration (FDA) and the European Medicines Agency (EMA) [6].

ICG is a near-infrared dye that binds to plasma proteins after intravenous or intra-cavity administration, making it ideal for visualizing vascular and tissue dynamics. Once illuminated with near-infrared light, it emits fluorescence that can be detected by specialized imaging systems, providing surgeons with critical information about blood flow, tissue perfusion, and anatomical landmarks. This real-time feedback is invaluable in pediatric urology, where precision is essential to avoid complications and preserve organ function. To perform MIS using ICG near-infrared fluorescence (NIRF), an ICG vial, along with specialized optics and cameras, is necessary [7, 8]. Many fluorescence imaging platforms are now commercially available and healthcare professionals should basically know their technical characteristics to optimize their use for each clinical indication [7]. In robotic-assisted surgery with the Da Vinci Xi platform, this technology is already incorporated into the system under the Firefly[®] module developed by Novadaq[®] Technologies Inc., Toronto, Canada [9].

ICG fluorescence imaging represents a significant leap forward in pediatric urology, bridging the gap between traditional surgical techniques and modern, image-guided interventions.

However, its application in the pediatric urology field is still in its early phase, currently corresponding to IDEAL Stage 2a [10]. Research conducted at this stage typically involves small-scale and observational studies, focusing on individual cases or small series. Key characteristics of IDEAL Stage 2a include the absence of formal control groups, reliance on descriptive data, and an exploratory approach aimed at refining techniques and assessing feasibility.

As evidence supporting its efficacy continues to grow, it is poised to become a cornerstone of surgical innovation, improving outcomes for children with complex urological conditions [11, 12]. Nonetheless, experience with ICG in the pediatric population is still limited [13-15].

This study aimed to evaluate the safety, efficacy, and

broader applications of ICG-guided fluorescence imaging in pediatric robotics and laparoscopy for urological indications, emphasizing its role in facilitating intraoperative anatomical navigation and enhancing decision-making during complex procedures. Building on our previous research on ICG applications, this work expands the focus to include a larger cohort and a diverse range of procedures to establish standardized protocols.

Methods

The records of all patients undergoing robotic or laparoscopic urological surgery with ICG-NIRF assistance over a 7-year period (2018–2024), were analyzed retrospectively.

For all indications except varicocele, prostatic utricle, PUD, and urachal cyst, ICG was administered intravenously. For these specific cases, the ICG solution was injected intraparenchymally or into the bladder. The administered dose ranged between 0.035 and 0.5 mg/kg. Laparoscopic surgeries were carried out using either the IMAGE1 S[™] or the IMAGE1 S[™] Rubina[®] system (KARL STORZ SE & Co. KG, Tuttlingen, Germany). Robotic surgeries utilized the da Vinci Xi robotic system (Intuitive Surgical, Sunnyvale, CA, USA) with a dual-console setup. The Firefly[®] technology facilitated seamless switching between standard bright light and ICG-NIRF imaging modes, ensuring precise visualization during surgery. Further details on the dosage and administration methods for specific indications are outlined below.

Operative procedures

Varicocelectomy

In laparoscopic procedures, one 10-mm optic port and two 5-mm working ports were inserted. In robotic procedures, three 8-mm robotic ports and a single 5-mm assistant port were placed, followed by docking the robotic system according to the pelvic setup. After dissecting the spermatic bundle, the ICG was injected into the body of the left testis using a 23-gauge needle. The dosage of ICG was adjusted based on the patient's weight. Patients weighing over 40 kg received a dose of 0.07 mg/kg, using a solution with a concentration of 2.5 mg/mL. For patients weighing less than 40 kg, a dose of 0.035 mg/kg was administered, also using a solution with a concentration of 2.5 mg/mL.

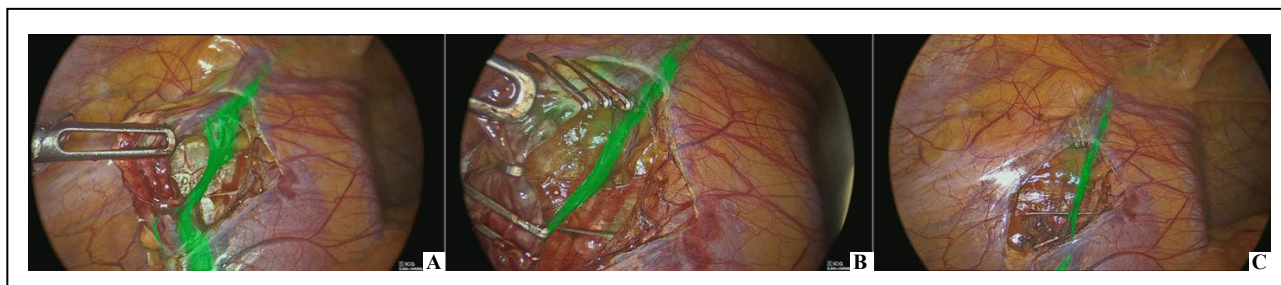


Figure 1. Laparoscopic varicocelectomy–lymphatics sparing on ICG-NIRF (A); clipping of spermatic vessels with lymphatics preservation (B); spared lymphatics after spermatic vessels division (C).

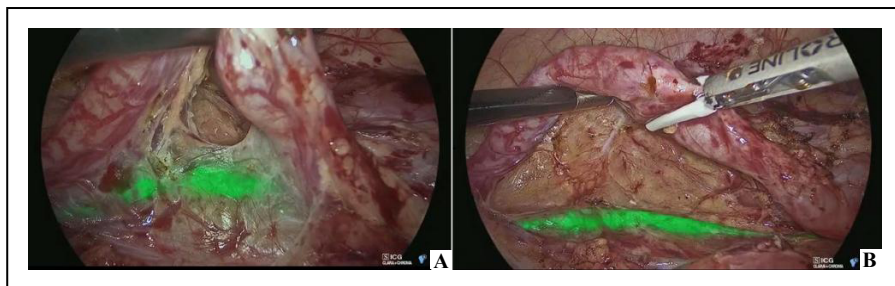


Figure 2. Laparoscopic partial nephrectomy—the normal ureter, containing an ICG solution injected through a ureteral catheter, appears fluorescent (A) using ICG-NIRF and can be clearly distinguished from the pathological ureter (B).

Once ICG-NIRF was activated, lymphatic vessels became fluorescent within 60 seconds of the intratesticular injection, enabling clear visualization. These lymphatic vessels were carefully dissected from the spermatic bundle and preserved. The subsequent steps, including clipping/ligating and sectioning the spermatic bundle in line with the Palomo procedure, were then successfully performed (Figure 1).

Pyeloplasty/nephrectomy/renal cyst removal

In laparoscopic procedures, one 10-mm optic port and either two or three 5-mm working ports were utilized. For robotic procedures, three 8-mm robotic ports and a single 5-mm assistant port were positioned, followed by docking the robotic system according to the specific lateral setup (right or left) for renal access.

After opening the Gerota fascia and before dissecting the renal hilum, a dose of 0.3 mg/kg ICG was administered intravenously via a peripheral vein using a solution with a concentration of 2.5 mg/mL. Within 30 to 120 seconds, the ICG-NIRF highlighted the renal vascular pedicle, providing valuable assistance in identifying vascular anomalies or crossing vessels, especially in cases with distorted anatomy caused by prior inflammation.

In cases involving simple renal cysts, ICG-NIRF facilitated visualization of the cyst dome, which displayed reduced fluorescence compared to the surrounding healthy renal parenchyma. This difference in fluorescence enabled a more precise and almost complete resection of the cyst roof, ensuring an anatomical approach to the procedure.

Partial nephrectomy

In laparoscopic procedures, one 10-mm optic port and either two or three 5-mm working ports were utilized. For robotic procedures, three 8-mm robotic ports and a single 5-mm assistant port were positioned, followed by docking the robotic system according to the specific lateral setup (right or left) for renal access.

In both surgical approaches, ICG was administered in three distinct phases to enhance visualization and guide the procedure.

- **First Injection:** 10 mL of ICG solution with a concentration of 2.5 mg/mL was delivered via a ureteral catheter, which had been placed through cystoscopy into the ureter of the normally functioning renal moiety. This allowed the normal ureter to fluoresce green under ICG-NIRF, enabling clear differentiation from the pathological and dilated ureter of the non-functioning moiety (Figure 2).

- **Second Injection:** A bolus of ICG (dose 0.3 mg/kg) using a solution with a concentration of 2.5 mg/mL was administered intravenously to initiate the angiographic phase. This step facilitated visualization of the main hilar vessels and the smaller vessels supplying the non-functioning renal moiety (Figure 3).

- **Third Injection:** Following the clipping and division of the vessels supplying the non-functioning renal moiety, another bolus of ICG (dose 0.3 mg/kg) using a solution with a concentration of 2.5 mg/mL was administered intravenously. This step served two purposes: it provided a clear demarcation line between the ischemic moiety to be removed (which appeared non-fluorescent) and the perfused healthy renal moiety (Figure 4), and it allowed assessment of the perfusion of the remaining functional moiety after parenchymal resection of the non-functioning renal pole (Figure 5).

Dismembered extravesical ureteral reimplantation and diverticulectomy

After establishing pneumoperitoneum and positioning the ports (three 8-mm robotic ports and one 5-mm assistant port), the robotic system was docked according to the pelvic-specific setup. ICG-NIRF was predominantly utilized in cases of complex primary obstructive megaureter (POM) associated with PUD.

For this indication, two separate ICG injections were performed:

- **First Injection:** 5-10 mL of ICG solution with a concentration of 2.5 mg/mL was injected through a ureteral catheter that had been placed via cystoscopy into the diverticulum. This step enabled precise visualization of the diverticulum's point of entry into the bladder, significantly

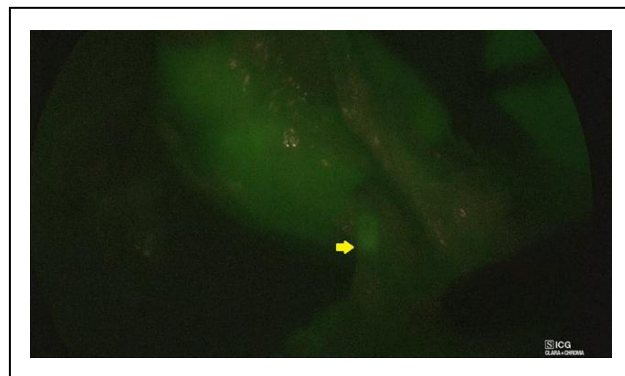


Figure 3. Laparoscopic partial nephrectomy—ICG-NIRF facilitated visualization of the small vessels supplying the non-functioning renal moiety.

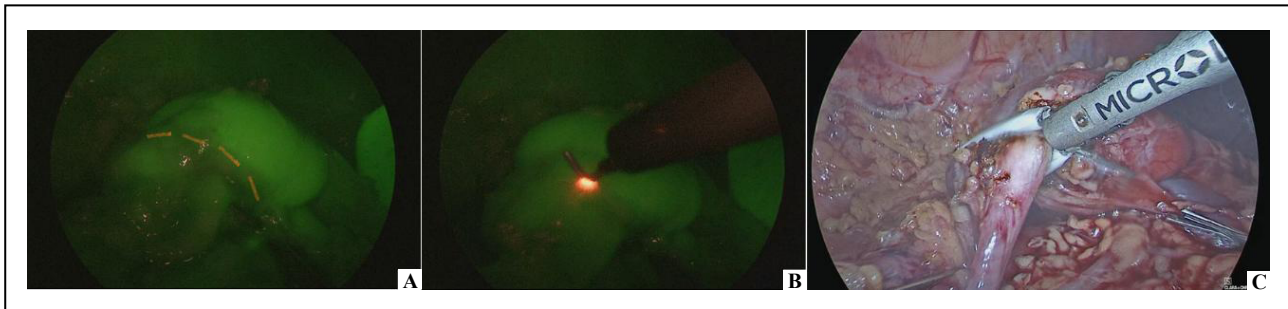


Figure 4. Laparoscopic partial nephrectomy–ICG-NIRF provided a clear demarcation line between the ischemic moiety (non-fluorescent) and the perfused healthy moiety (fluorescent) (A-B) and aided the parenchymal resection (C).

aiding in its dissection and ligation.

- **Second Injection:** Following the detachment of the dilated ureter from the bladder and subsequent ureteral tapering, a bolus of ICG (dose 0.3 mg/kg) using a solution with a concentration of 2.5 mg/mL was administered intravenously. This allowed for the evaluation of ureteral perfusion, ensuring adequate blood supply to the reconstructed ureter.

Resection of adnexal pathology

In laparoscopic procedures, one 10-mm optic port and two 5-mm working ports were utilized. For robotic procedures, three 8-mm robotic ports and a single 5-mm assistant port were positioned, followed by docking the robotic system over the patient's feet, aligning with the pelvic (gynecologic) specific setup.

During the procedure, a dose of 0.5 mg/kg ICG was administered intravenously using a solution with a concentration of 2.5 mg/mL. Fluorescence became evident in the target organs in approximately 60 seconds, aiding in the identification of resection margins and the assessment of tissue perfusion. ICG-NIRF was specifically utilized in cases of ovarian masses to delineate resection margins and assist intraoperative decision-making (Figure 6).

Additionally, in cases of adnexal torsion or paratubal lesions, ICG-NIRF was employed to evaluate perfusion patterns both before and after detorsion or excision. This provided crucial information to support decisions for conservative management when feasible (Figure 7).

Excision of prostatic utricle cyst

Initial cystourethroscopy confirmed the presence of the utricular remnant and identified its orifice on the verumontanum. A ureteral catheter was then placed into the utricu-

lar cyst and left in situ. After placing the ports—three 8-mm robotic ports and one 5-mm assistant port—the robotic system was docked following the pelvic-specific setup. At this stage, 2.5-3 mL of ICG solution with a concentration of 2.5 mg/mL were injected directly into the utricular cyst via the ureteral catheter. This injection enabled ICG-guided fluorescence imaging, which provided enhanced visualization of the cyst. This facilitated its careful dissection between the bladder and rectum using monopolar and bipolar energy for precise and safe separation, ensuring secure ligation of its connection to the urethra. Once freed from the surrounding tissues, the neck of the cyst was ligated with a loop and excised. The cyst was then removed through the umbilical port, completing the procedure.

Excision of urachal remnant

Before initiating the surgery, the bladder was filled with approximately 150 mL of ICG solution with a concentration of 0.8 mg/mL. A 10-mm trocar was inserted for a 0-degree laparoscope, along with two additional 5-mm working trocars positioned in the left and right upper abdominal quadrants. The urachal remnant was identified along its entire length, extending from the umbilicus to the bladder dome. The peritoneum overlaying the cyst was incised using either monopolar scissors or an energy device. Dissection began midway between the umbilicus and the bladder dome to locate the median umbilical ligament. The cyst was dissected in the direction of the umbilicus, and its attachment was either ligated or divided. Subsequently, the dissection continued toward the supravescical portion of the cyst. During this step, near-infrared fluorescence provided excellent visualization through the bladder wall, which had been filled with ICG solution. This enhanced visibility helped prevent accidental bladder injury

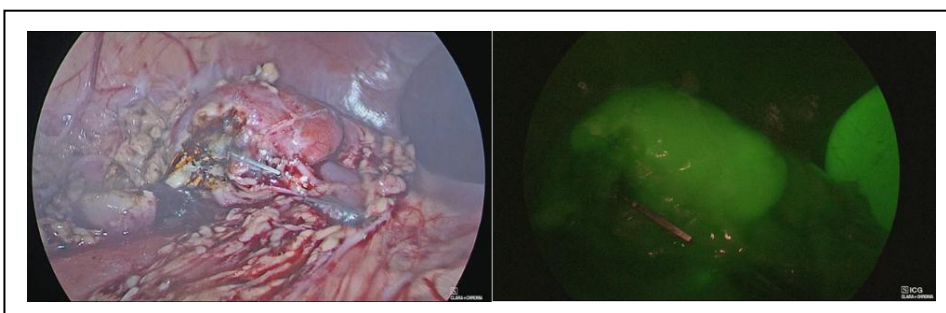


Figure 5. Laparoscopic partial nephrectomy–ICG-NIRF was helpful to assess perfusion of the remaining functional moiety after parenchymal resection of the non-functioning renal pole.

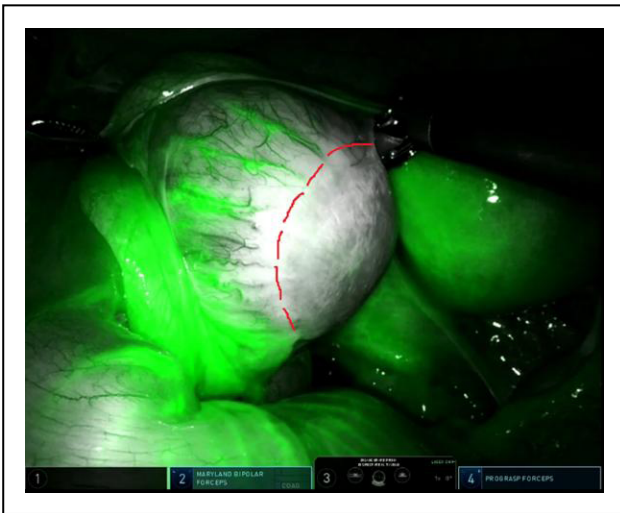


Figure 6. Ovarian mass–ICG-NIRF allowed to assess the resection margin and decide for ovarian sparing surgery.

during dissection. The cyst was then excised along with a small segment of the bladder dome, and the opening was closed proximally using a 2/0 endoloop (Figure 8).

To further secure the closure, a 2/0 transfixed suture was placed, with knots tied on both the anterior and posterior sides of the bladder. Once the cyst was removed, the integrity of the bladder closure was verified by instilling saline through the bladder catheter while observing laparoscopically for potential leaks. The excised cyst and associated tissue were extracted via the umbilical incision.

Results

The patient cohort consisted of 278 patients (192 boys and 86 girls), with median age of 9.2 years (range 1-18). Of these, 181 patients (65.1%) underwent laparoscopic procedures with ICG-NIRF guidance, including pyeloplasty ($n = 11$), varicocelelectomy ($n = 118$), adnexal pathology resection ($n = 33$), partial nephrectomy ($n = 10$), nephrectomy ($n = 6$), and urachal cyst excision ($n = 3$). The remaining 97 patients (34.9%) underwent robot-assisted procedures, which included pyeloplasty ($n = 22$), varicocelelectomy ($n = 34$), adnexal pathology resection ($n = 17$), partial nephrectomy ($n = 4$), nephrectomy ($n = 4$), excision of periureteral diverticulum (PUD), ureteral dismembering and extravesical ureteral reimplantation ($n =$

13), renal cyst removal ($n = 2$), and prostatic utricle cyst excision ($n = 1$).

All procedures were completed successfully without conversions to open surgery. The median time for robot docking was 12 minutes, ranging from 5 to 26 minutes. For intraoperative ICG-NIRF visualization, patients undergoing Palomo varicocelelectomy had a median lymphatic visualization time of 60 seconds (range 30-120) after intratesticular injection. The lymphatics remained clearly visible for 5 to 7 minutes before the dye diffused into the spermatic artery and veins, at which point lymphatic visibility decreased. The time required to preserve the lymphatics ranged between 1 and 4 minutes, enabling successful lymphatic sparing in all cases. In renal procedures involving intravenous dye administration, the median time for target organ visualization was 60 seconds, with a range of 30 to 120 seconds post-injection. In trans-catheter injections, ICG-NIRF was instantly visible in structures such as the ureter, bladder, diverticulum, or utricle remnant. In gynecological procedures, fluorescence appeared in ovary or fallopian tube in approximately 60 seconds (range 40-80) following the injection. The adnexal masses typically appeared hypo-fluorescent compared to the surrounding ovarian parenchyma. Histopathology confirmed the diagnosis of immature teratoma ($n = 7$), mature teratoma ($n = 6$), mucinous cystadenoma ($n = 2$), theco-fibroma ($n = 1$), granulosa cell tumor ($n = 1$).

There were no allergic or anaphylactic reactions to ICG. Clear visualization of target anatomy was achieved in all cases, with no intraoperative complications. The median hospital stay was 2.7 days, ranging from 1 to 7 days. Regarding postoperative complications, hemoperitoneum caused by bleeding from a parietal vessel occurred in a 17-year-old patient after robotic Palomo varicocelelectomy (Clavien 3b). This required reoperation 48 hours later to evacuate the hemoperitoneum and control the bleeding. Another case involved a 5-year-old boy who experienced double-J stent dislodgement following robot-assisted pyeloplasty (Clavien 3b). Ureteroscopy was performed three days after the initial surgery to remove the displaced stent and replace it with a new one.

Regarding functional outcomes, after varicocelelectomy, no varicocele recurrence or postoperative hydrocele was observed in patients operated on using both approaches. Similarly, no loss of function of the residual kidney moiety was observed on renal scans at 1-year follow up in all patients undergoing laparoscopic or robot-assisted partial

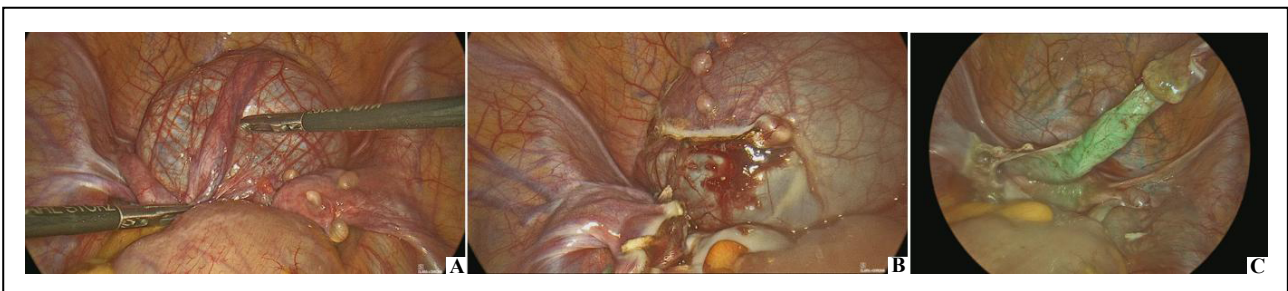


Figure 7. Laparoscopic removal of giant paratubal lesion—following the removal of the paratubal lesion (A-B), ICG-NIRF aided to assess the perfusion pattern of the fallopian tube (C).

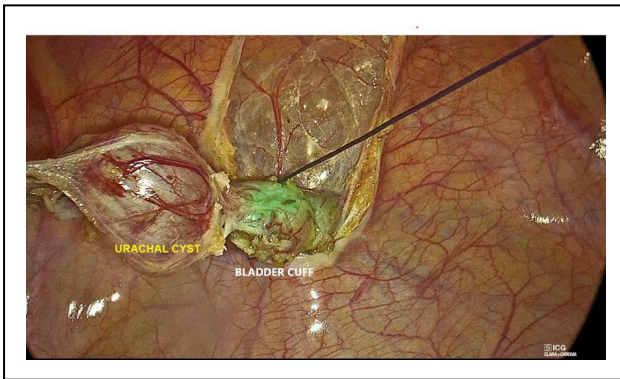


Figure 8. Laparoscopic removal of urachal remnant–ICG-NIRF allowed to visualize the bladder dome and remove the urachal cyst along with a small cuff of the bladder dome using an endoloop.

nephrectomy. In cases of pyeloplasty, a significant reduction in antero-posterior diameter (median 11.7 mm, range 0-22 mm) was observed at 1-year follow-up compared to preoperative values (median 33.8 mm, range 28-70 mm). Patient demographics and outcome parameters of laparoscopic and robotic approaches are reported in Table 1 and Table 2, respectively.

Discussion

The primary objective of any surgical procedure is to achieve the best possible outcomes by ensuring precise visualization and identification of key anatomical structures. ICG fluorescence has emerged as a valuable adjunct

in this context, enhancing visibility in pediatric urological procedures [1-3]. In pyeloplasty, for instance, it aids in confirming the viability of the renal pelvis and ensuring proper anastomosis of the ureter [16, 17]. Similarly, during nephron-sparing surgeries, ICG-NIRF enables delineation of tumor margins and preservation of healthy renal parenchyma, which are crucial for maintaining long-term renal function [18, 19]. Its application in complex reconstructive surgeries, such as cases involving ectopic ureters, highlights its potential to visualize structures that are challenging to identify using conventional techniques [20, 21].

A significant advantage of ICG-guided fluorescence lies in its role as a non-ionizing alternative to intraoperative imaging, reducing reliance on fluoroscopy and minimizing radiation exposure, particularly in young patients. This technology, facilitating minimally invasive and robot-assisted surgeries, contributes to faster recovery times, reduced postoperative pain, and shorter hospital stays [2, 22-24]. Moreover, its biocompatibility, rapid clearance, and absence of significant side effects make it particularly well-suited for pediatric patients [2, 23]. These advantages align with the principles of precision medicine and minimally invasive surgery, emphasizing safety and patient-centric outcomes.

In our clinical practice, we have integrated ICG fluorescence technology into minimally invasive surgery (MIS) protocols, yielding consistently favorable outcomes. Established protocols for ICG administration, including timing, dosage, and delivery methods, have facilitated its application across various indications [3, 5]. One prominent application is in the management of varico-

Table 1. Patient demographics and outcome parameters of laparoscopic approaches.

Parameter	Varicocelectomy	Pyeloplasty	Nephrectomy	Partial nephrectomy	Resection of adnexal pathology	Excision of urachal cyst
Patients, <i>n</i>	118	11	6	10	33	3
M/F, <i>n/n</i>	118/0	6/5	2/4	5/5	0/33	2/1
Median age, years (range)	14.1 (11-16)	4.3 (1-7)	10.6 (8-12)	5.1 (3-7)	14.3 (11-15)	9.1 (4-12)
Median weight, kg (range)	59.5 (40-65)	19.4 (13.8-28)	41.6 (32-55)	23.1 (19-29)	50.9 (38-60)	26.6 (21-36)
Operative time, min (range)	24.6 (15-39)	105 (84-150)	66 (55-80)	95 (78-130)	38 (21-70)	51 (40-69)
Intra-operative complications, <i>n</i>	0	0	0	0	0	0
Conversion, <i>n</i>	0	0	0	0	0	0
ICG administration	Intratesticular	Intravenous	Intravenous	Trans-catheter 2) Intravenous	Intravenous	Trans-catheter
Timing of ICG-NIRF	60 (30-120)	60 (30-120)	60 (30-120)	60 (30-120)	60 (40-80)	0
Post-operative complications, <i>n</i>	0	0	0	0	0	0
Median LOS, days (range)	1.1 (0-1.5)	3.5 (3-5)	2.3 (2-4)	3.5 (2-5)	1.3 (1-2)	2.1 (2-4)
Allergy or systemic adverse reaction to ICG, <i>n</i> (%)	0	0	0	0	0	0

Note: LOS = length of stay.

Table 2. Patient demographics and outcome parameters of robotic approaches.

Parameter	Vari-coelectomy	Pyeloplasty	Renal cyst removal	Nephrectomy	Partial nephrectomy	PUD excision + dismembered ureteral reimplantation	Resection of adnexal pathology	Excision of prostatic utricle cyst
Patients, <i>n</i>	34	22	2	4	4	13	17	1
M/F, <i>n/h</i>	34/0	8/14	2/0	2/2	1/3	12/1	0/17	1/0
Median age, years (range)	17.3 (16-18)	5.1 (3-9)	8.5 (7-15)	16.4 (11-16)	5.7 (3-7)	6.7 (5-11)	17.3 (14-17)	4
Median weight, kg (range)	79.5 (72-90)	25.6 (13.8-35)	38 (28-67)	60.4 (32-68)	34.3 (24-38)	33.6 (25-48)	62.3 (55-69)	20
Total operative time, min (range)	34.5 (30-46)	123 (95-180)	75 (64-89)	85 (70-95)	110 (87-155)	106 (96-170)	47 (23-68)	115
Docking time, min (range)	10 (5-15)	16 (13-26)	13.5 (14-21)	11.5 (12-20)	12.5 (9-18)	10.3 (8-15)	11.2 (9-17)	11
Intra-operative complications, <i>n</i> (%)	0	0	0	0	0	0	0	0
Conversion, <i>n</i>	0	0	0	0	0	0	0	0
ICG administration route	Intrastreticular	Intravenous	Intravenous	Intravenous	Trans-catheter 2) Intravenous	Trans-catheter 2) Intravenous	Intravenous	Trans-catheter
Timing of ICG-NIRF visualization, seconds (range)	60 (30-120)	60 (30-120)	60 (30-120)	60 (30-120)	60 (30-120)	0	60 (40-80)	0
Post-operative complications, <i>n</i> (%)	1 (2.9)	1 (4.5)	0	0	0	0	0	0
Median LOS, days (range)	1.1 (0-1.5)	4.0 (3-7)	2.3 (2-4)	2.1 (2-4)	2.7 (2-4)	2.7 (2-4)	1.3 (1-2)	2.5
Allergy or systemic adverse reaction to ICG, <i>n</i> (%)	0	0	0	0	0	0	0	0

Note: PUD = periureteral diverticulum; LOS = length of stay.

cele, where the laparoscopic lymphatic sparing Palomo procedure is a standard approach in pediatric patients [25]. In such indication, the ICG dye is administered via intra- or para-testicular injection, leading to equally good visualization of lymphatic vessels with minimal risk of testicular injuries [26, 27]. Robotic-assisted varicocelectomy further enhances precision, eliminating the need for surgical clips by enabling efficient ligation of spermatic vessels [28, 29]. In selecting the surgical approach for patients with varicocele, we preferentially opted for the robotic approach in patients weighing over 70 kg, primarily to avoid the use of large 12 mm clips for closing large vessels. Adopting ligatures for spermatic cord ligation is less time-consuming and technically demanding in robotics rather than in laparoscopy. The median operative time for laparoscopic varicocelectomy was 24.6 minutes (range 15–39), while it was 34.5 minutes (range 30–46) for robotic approach. However, as the docking time, averaging 10 minutes (range 5–15), was included in the total operative time of the robotic procedure, no significant difference in operative time was observed between laparoscopic and robotic approaches. Additionally, no extra material costs were associated with the robotic approach, apart from the consumables required for the robotic kit. By adopting ligatures instead of clips, costs were further reduced, as ligatures are significantly less expensive than clip applicators. No associated anesthesiologic complications were observed during these procedures.

ICG fluorescence has also proven effective in partial nephrectomy, involving three injections: the first through a ureteral catheter to distinguish normal ureteral structures, the second intravenously to visualize vascular supply, and the third to delineate resection boundaries. This approach ensures accurate preservation of functional renal tissue while removing pathological portions [30, 31].

For nephrectomy, ICG fluorescence facilitates identification of renal vessels, even in challenging cases involving severe adhesions or anatomical alterations due to prior inflammation. ICG fluorescence allows to visualize the dome of giant renal cysts, which do not fluoresce after injection [32, 33]. In pyeloplasty for ureteropelvic junction obstruction, ICG fluorescence is particularly valuable when there is suspicion of extrinsic obstruction caused by crossing vessels. It highlights the renal vascular pedicle, making it easier to identify vascular anomalies or crossing vessels, even in anatomies altered by prior inflammation. Moreover, it ensures proper vascularization of the ureter following isolation and spatulation, providing critical guidance before the anastomosis is performed.

Regarding functional outcomes, after varicocelectomy, no varicocele recurrence or postoperative hydrocele was observed in patients operated on using both approaches. Similarly, no loss of function of the residual kidney moiety was observed on renal scans at 1-year follow up in all patients undergoing laparoscopic or robot-assisted partial nephrectomy. In cases of pyeloplasty, a significant reduction in antero-posterior diameter was observed at 1-year follow-up compared to preoperative values.

For pathologies involving the bladder, ureter, and urethra,

ICG fluorescence enhances surgical precision. In cases of prostatic utricle, injecting ICG through a ureteral catheter into the utricle produces green fluorescence, guiding the robotic dissection. Similarly, in bladder diverticula, ICG can be injected into the diverticulum to aid dissection. In ureteral reimplantation, ICG fluorescence is employed to assess ureteral vascularization, particularly in cases involving megaureters that require tapering before reimplantation into the bladder. In cases of urachal remnants, ICG-NIRF proved highly effective during cyst dissection, providing clear visualization of the bladder dome, and helping to prevent injury.

In pediatric and adolescent gynecology, ICG fluorescence imaging has proven useful for both cancer and non-cancer conditions [34]. Regarding oncological applications, the adnexal masses typically appeared hypo-fluorescent compared to the surrounding ovarian parenchyma. Histopathology confirmed the diagnosis of immature teratoma, mature teratoma, mucinous cystadenoma, theco-fibroma, and granulosa cell tumor. The lack of avidity for ICG observed in such tumors was probably related to absence of enhanced permeability and retention (EPR) effects, characteristic of specific tumor pathophysiologies, and considered prerequisites for fluorescence detection [35]. However, its utility in detecting neoplastic lesions should be further validated, considering the limited data on its specificity and sensitivity for various tumor types.

In gynecological emergencies such as ovarian torsion, ICG fluorescence highlights the ovarian vascular network, aiding in both diagnosis and post-detorsion assessment of organ viability [36–38].

Despite these benefits, there are important limitations and considerations. From a cost perspective, while the price of an ICG vial (approximately €40) is relatively modest, the investment in imaging systems is substantial. The initial cost of acquiring fluorescence-capable laparoscopic or robotic platforms can range from tens to hundreds of thousands of euros, depending on the system's features and capabilities. This cost can be prohibitive in certain settings, particularly in smaller or resource-limited hospitals. However, when weighed against the potential savings from shorter hospital stays, reduced complications, and faster recovery times, the technology may prove cost-effective over the long term. Additionally, reconstituted ICG vials can be utilized for multiple procedures within their stability window, optimizing resource use. Efforts to lower the cost of imaging platforms through technological innovation could further enhance accessibility. Moreover, manufacturers could explore rental models or bundled pricing strategies to facilitate adoption by institutions with limited capital budgets.

The safety profile of ICG has been well documented, with no significant systemic or local adverse effects reported in our clinical experience. However, rare allergic reactions, including mild cutaneous manifestations and, in extremely rare cases, anaphylaxis, have been observed and must be anticipated and managed appropriately [39, 40]. These reactions necessitate preoperative screening for known iodine or shellfish allergies, as ICG is iodine-based. Further-

more, careful monitoring during administration is essential to detect and address adverse effects promptly. ICG's rapid clearance from the body and its biocompatibility make it a preferred choice for pediatric applications, but vigilance remains critical to ensure patient safety.

The learning curve for this technology needs to be further elaborated, particularly regarding the specific roles of the surgical team. For instance, while the surgeon must familiarize themselves with interpreting fluorescence imaging, the anesthetist's role in administering the dye typically involves straightforward protocols that require minimal additional training. This division of responsibilities suggests that the overall learning curve may not be as steep as initially perceived. Moreover, surgical staff can leverage existing training programs and simulation tools to accelerate the adoption of ICG fluorescence technology, ensuring a more efficient integration into routine clinical practice.

Technological advancements addressing the limitations of current systems, such as black-and-white transitions in imaging modes, are necessary to enhance usability and provide a more intuitive experience for surgeons.

This study is not without limitations. The retrospective nature of the analysis introduces inherent biases, and the absence of a control group restricts the ability to draw definitive conclusions regarding the efficacy of ICG fluorescence. Further prospective, controlled studies with larger cohorts are essential to validate these preliminary observations and refine the application of ICG technology in pediatric urology.

Conclusions

The findings of this study highlight the potential of ICG fluorescence as an innovative tool in the pediatric urology field. While the current evidence supports its safety, feasibility, and ability to enhance intraoperative visualization, the study's exploratory nature necessitates further research. Prospective, controlled trials are needed to validate its efficacy, investigate long term functional outcomes, and compare its utility with existing standard practices. Until these data are available, ICG fluorescence should be considered a promising adjunct rather than a standard of care. While its application in specific procedures, such as partial nephrectomy, varicocele repair, and ureteral reconstruction, demonstrated its versatility, safety, and potential to improve surgical precision, further research is required to optimize its applications and address its limitations.

Declarations

Author contributions: Esposito C, Escolino M, Di Mento C, Chiodi A, Carraturo F made substantial contributions to conception and design of the study and performed data analysis and interpretation; Del Conte F, Cerulo M, Coppola V, Tedesco F, Esposito G, Mazzone V performed data acquisition, as well as provided administrative, technical, and material support. All authors read and approved the

final manuscript.

Availability of data and materials: Data will be available on reasonable request.

Financial support and sponsorship: None.

Conflicts of interest: All authors declare that there are no conflicts of interest.

Ethical approval and informed consent: Not applicable.

Consent for publication: Not applicable.

References

1. Zeineddin S, Linton S, Inge M, De Boer C, Hu A, Goldstein SD, *et al.* Fluorescence-guided surgery: national trends in adoption and application in pediatric surgery. *J Pediatr Surg*, 2023, 58(4): 689-694. [[Crossref](#)]
2. Szavay PO, Bondoc A, Esposito C, Goldstein SD, Harms M, Kowalewski G, *et al.* Clinical consensus statement on the use of indocyanine green fluorescence-guided surgery in pediatric patients. *J Pediatr Surg*, 2024, 59(11): 1616-1657. [[Crossref](#)]
3. Esposito C, Del Conte F, Cerulo M, Gargiulo F, Izzo S, Esposito G, *et al.* Clinical application and technical standardization of indocyanine green (ICG) fluorescence imaging in pediatric minimally invasive surgery. *Pediatr Surg Int*, 2019, 35(10): 1043-1050. [[Crossref](#)]
4. Fernández-Bautista B, Mata DP, Parente A, Pérez-Caballero R, & De Agustín JC. First experience with fluorescence in pediatric laparoscopy. *European J Pediatr Surg Rep*, 2019, 7(1): e43-e46. [[Crossref](#)]
5. Esposito C, Coppola V, Del Conte F, Cerulo M, Esposito G, Farina A, *et al.* Near-Infrared fluorescence imaging using indocyanine green (ICG): emerging applications in pediatric urology. *J Pediatr Urol*, 2020, 16(5): 700-707. [[Crossref](#)]
6. Esposito C, Borgogni R, Autorino G, Cerulo M, Carulli R, Esposito G, *et al.* Applications of indocyanine green-guided near-infrared fluorescence imaging in pediatric minimally invasive surgery urology: a narrative review. *J Laparoendosc Adv Surg Tech A*, 2022, 32(12): 1280-1287. [[Crossref](#)]
7. Preziosi A, Cirelli C, Waterhouse D, Privitera L, De Coppi P, & Giuliani S. State of the art medical devices for fluorescence-guided surgery (FGS): technical review and future developments. *Surg Endosc*, 2024, 38(11): 6227-6236. [[Crossref](#)]
8. Dalli J, Jindal A, Gallagher G, Epperlein JP, Hardy NP, Mallallah R, *et al.* Evaluating clinical near-infrared surgical camera systems with a view to optimizing operator and computational signal analysis. *J Biomed Opt*, 2023, 28(3): 035002. [[Crossref](#)]
9. Esposito C, Settini A, Del Conte F, Cerulo M, Coppola V, Farina A, *et al.* Image-guided pediatric surgery using indocyanine green (ICG) fluorescence in laparoscopic and robotic surgery. *Front Pediatr*, 2020, 8: 314-324. [[Crossref](#)]
10. Preziosi A, Paraboschi I, & Giuliani S. Evaluating the de-

- velopment status of fluorescence-guided surgery (FGS) in pediatric surgery using the idea, development, exploration, assessment, and long-term study (IDEAL) framework. *Children*, 2023, 10(4): 689-699. [Crossref]
11. Iacob ER, Iacob R, Ghenciu LA, Popoiu TA, Stoicescu ER, & Popoiu CM. Small scale, high precision: robotic surgery in neonatal and pediatric patients-a narrative review. *Children*, 2024, 11(3): 270-280. [Crossref]
 12. Esposito C, Autorino G, Castagnetti M, Cerulo M, Coppola V, Cardone R, et al. Robotics and future technical developments in pediatric urology. *Semin Pediatr Surg*, 2021, 30(4): 151082. [Crossref]
 13. Paraboschi I, Mantica G, Minoli DG, De Marco EA, Gnech M, Bebi C, et al. Fluorescence-guided surgery and novel innovative technologies for improved visualization in pediatric urology. *Int J Environ Res Public Health*, 2022, 19(18): 11194. [Crossref]
 14. Privitera L, Paraboschi I, Dixit D, Arthurs OJ, & Giuliani S. Image-guided surgery and novel intraoperative devices for enhanced visualisation in general and paediatric surgery: a review. *Innov Surg Sci*, 2021, 6(4): 161-172. [Crossref]
 15. Paraboschi I, De Coppi P, Stoyanov D, Anderson J, & Giuliani S. Fluorescence imaging in pediatric surgery: State-of-the-art and future perspectives. *J Pediatr Surg*, 2021, 56(4): 655-662. [Crossref]
 16. Petrut B, Bujoreanu CE, Porav Hodade D, Hardo VV, Ovidiu Coste B, Maghiar TT, et al. Indocyanine green use in urology. *J buon*, 2021, 26(1): 266-274.
 17. Pathak RA, & Hemal AK. Intraoperative ICG-fluorescence imaging for robotic-assisted urologic surgery: current status and review of literature. *Int Urol Nephrol*, 2019, 51(5): 765-771. [Crossref]
 18. Abdelhafeez AH, Murphy AJ, Brennan R, Santiago TC, Lu Z, Krasin MJ, et al. Indocyanine green-guided nephron-sparing surgery for pediatric renal tumors. *J Pediatr Surg*, 2022, 57(9): 174-178. [Crossref]
 19. Pio L, Wijnen M, Giuliani S, Sarnacki S, Davidoff AM, & Abdelhafeez AH. Identification of pediatric tumors intraoperatively using indocyanine green (ICG). *Ann Surg Oncol*, 2023, 30(12): 7789-7798. [Crossref]
 20. Mandovra P, Kalikar V, & Patankar RV. Real-time visualization of ureters using indocyanine green during laparoscopic surgeries: can we make surgery safer? *Surg Innov*, 2019, 26(4): 464-468. [Crossref]
 21. Lee Z, Moore B, Giusto L, & Eun DD. Use of indocyanine green during robot-assisted ureteral reconstructions. *Eur Urol*, 2015, 67(2): 291-298. [Crossref]
 22. Cacciamani GE, Shakir A, Tafuri A, Gill K, Han J, Ahmadi N, et al. Best practices in near-infrared fluorescence imaging with indocyanine green (NIRF/ICG)-guided robotic urologic surgery: a systematic review-based expert consensus. *World J Urol*, 2020, 38(4): 883-896. [Crossref]
 23. Sincavage J, Gulack BC, & Zamora IJ. Indocyanine green (ICG) fluorescence-enhanced applications in pediatric surgery. *Semin Pediatr Surg*, 2024, 33(1): 151384. [Crossref]
 24. Fransvea P, Miccini M, Rondelli F, Brisinda G, Costa A, Garbarino GM, et al. A green lantern for the surgeon: a review on the use of indocyanine green (ICG) in minimally invasive surgery. *J Clin Med*, 2024, 13(16): 4895-4903. [Crossref]
 25. Esposito C, Turrà F, Del Conte F, Izzo S, Gargiulo F, Farina A, et al. Indocyanine green fluorescence lymphography: a new technique to perform lymphatic sparing laparoscopic palomo varicocelectomy in children. *J Laparoendosc Adv Surg Tech A*, 2019, 29(4): 564-567. [Crossref]
 26. Esposito C, Borgogni R, Chiodi A, Cerulo M, Autorino G, Esposito G, et al. Indocyanine green (ICG)-GUIDED lymphatic sparing laparoscopic varicocelectomy in children and adolescents. Is intratesticular injection of the dye safe? A mid-term follow-up study. *J Pediatr Urol*, 2024, 20(2): 282.e281-282.e286. [Crossref]
 27. Zundel S, & Szavay P. Para-testicular injection of indocyanine green for laparoscopic immunofluorescence-guided lymphatic-sparing Palomo procedure: promising preliminary results. *J Pediatr Urol*, 2024, 20(3): 530-532. [Crossref]
 28. Esposito C, Leva E, Castagnetti M, Cerulo M, Cardarelli M, Del Conte F, et al. Robotic-assisted versus conventional laparoscopic ICG-fluorescence lymphatic-sparing palomo varicocelectomy: a comparative retrospective study of techniques and outcomes. *World J Urol*, 2024, 42(1): 215-225. [Crossref]
 29. Reinhardt S, Thorup J, Joergensen PH, & Fode M. Robot-assisted laparoscopic varicocelectomy in a pediatric population. *Pediatr Surg Int*, 2023, 39(1): 202-212. [Crossref]
 30. Herz D, DaJusta D, Ching C, & McLeod D. Segmental arterial mapping during pediatric robot-assisted laparoscopic heminephrectomy: a descriptive series. *J Pediatr Urol*, 2016, 12(4): 266.e261-266. [Crossref]
 31. Esposito C, Autorino G, Coppola V, Esposito G, Paternoster M, Castagnetti M, et al. Technical standardization of ICG near-infrared fluorescence (NIRF) laparoscopic partial nephrectomy for duplex kidney in pediatric patients. *World J Urol*, 2021, 39(11): 4167-4173. [Crossref]
 32. Licari LC, Bologna E, Proietti F, Flammia RS, Bove AM, D'Annunzio S, et al. Exploring the applications of indocyanine green in robot-assisted urological surgery: a comprehensive review of fluorescence-guided techniques. *Sensors*, 2023, 23(12): 5497-5502. [Crossref]
 33. Esposito C, Soria-Gondek A, Castagnetti M, Cerulo M, Del Conte F, Esposito G, et al. Laparoscopic or robotic deroofting guided by indocyanine green fluorescence and perirenal fat tissue wadding technique of pediatric simple renal cysts. *J Laparoendosc Adv Surg Tech A*, 2020, 30(4): 471-476. [Crossref]
 34. Esposito C, Blanc T, Di Mento C, Ballouhey Q, Fourcade L, Mendoza-Sagaon M, et al. Robotic-assisted surgery for gynecological indications in children and adolescents: European multicenter report. *J Robot Surg*, 2024, 18(1): 20-31. [Crossref]
 35. Wang Y, Zhang Y, Li M, Gao X, & Su D. An efficient strategy for constructing fluorescent nanoprobe for prolonged and accurate tumor imaging. *Anal Chem*, 2024, 96(6): 2481-2490. [Crossref]
 36. Nicholson K, Urh A, Demertzis K, Holubyeva A, LaPier Z,

- Cisneros-Camacho A, *et al.* Intraoperative indocyanine green dye use in ovarian torsion: a feasibility study. *J Minim Invasive Gynecol*, 2022, 29(6): 738-742. [[Crossref](#)]
37. Plöger R, Condic M, Ralser DJ, Plöger HM, Egger EK, Otten LA, *et al.* Intraoperative utilization of indocyanine green (ICG) dye for the assessment of ovarian perfusion—case report and review of the literature. *J Clin Med*, 2023, 12(18): 5923-5933. [[Crossref](#)]
38. Lorenzo GD, Mirenda G, Gentile RM, Pozzolo CD, De Santo D, Romano F, *et al.* Use of indocyanine green to evaluate ovarian perfusion after laparoscopic detorsion. A step-by-step demonstration video. *J Minim Invasive Gynecol*, 2024, 31(4): 269-270. [[Crossref](#)]
39. Sasaki M, & Murata Y. Anaphylaxis induced by indocyanine green during abdominal surgery: a case report. *Saudi J Anaesth*, 2024, 18(4): 590-592. [[Crossref](#)]
40. Keller NB, Stapler SM, Shanker BA, & Cleary RK. Anaphylactic shock to intravenous indocyanine green during a robotic right colectomy. *Am Surg*, 2023, 89(12): 6407-6409. [[Crossref](#)]

Cite this article as: Esposito C, Cerulo M, Carraturo F, Del Conte F, Di Mento C, *et al.* Use of ICG-guided fluorescence imaging in pediatric laparoscopic and robot-assisted surgery: a single-center retrospective study. *Uro-Technology Journal*, 2025, 9(1): 01-11. doi: 10.31491/UTJ.2025.03.030